University of Nebraska - Lincoln
DigitalCommons@University of Nebraska - Lincoln

Marjorie A. Langell Publications | Published Research - Department of Chemistry

5-1-1996

High resolution electron energy loss spectroscopy of MnO(100) and oxidized MnO(100)

Marjorie Langell
University of Nebraska - Lincoln, mlangell1@unl.edu

C.W. Hutchings
University of Nebraska - Lincoln

G.A. Carson
University of Nebraska - Lincoln

M.H. Nassir
University of Nebraska - Lincoln

Follow this and additional works at: http://digitalcommons.unl.edu/chemistrylangell

Part of the Chemistry Commons

Langell, Marjorie ; Hutchings, C.W.; Carson , G.A.; and Nassir, M.H., "High resolution electron energy loss spectroscopy of MnO(100) and oxidized MnO(100)" (1996). *Marjorie A. Langell Publications.* Paper 8.
http://digitalcommons.unl.edu/chemistrylangell/8

This Article is brought to you for free and open access by the Published Research - Department of Chemistry at DigitalCommons@University of Nebraska - Lincoln. It has been accepted for inclusion in Marjorie A. Langell Publications by an authorized administrator of DigitalCommons@University of Nebraska - Lincoln.

High resolution electron energy loss spectroscopy of MnO(100) and oxidized MnO(100)

M. A. Langell, C. W. Hutchings, G. A. Carson, and M. H. Nassir
Department of Chemistry, University of Nebraska, Lincoln, Nebraska 68588-0304

(Received 12 October 1995; accepted 4 March 1996)

Single crystal MnO(100) substrates can be selectively oxidized to produce Mn_2O_3- and Mn_3O_4-like surfaces under mild oxidation/reduction conditions readily accessed under ultrahigh vacuum (UHV). MnO(100) yields a characteristic Mn 2*p* x-ray photoelectron spectroscopy (XPS) satellite structure and appropriate O/Mn concentrations from O 1*s*/Mn 2*p* XPS intensity ratios. Its high resolution electron energy loss (HREEL) spectrum shows a series of Fuchs–Kliewer multiple phonon excitations with a single loss energy of 70.9 meV, characteristic of the cubic manganese monoxide structure. However, the HREEL spectral (HREELS) background is high and the phonons are not as well resolved as those typically observed on comparable metal monoxides. Annealing the MnO(100) substrate at 625 K and 5×10^{-7} Torr O_2 slowly forms Mn_2O_3, as indicated by O 1*s* and Mn 2*p* XPS, and does so without significantly altering the symmetry of the MnO(100) low energy electron diffraction pattern. The MnO(100)-Mn_2O_3 surface can be selectively reduced to Mn_3O_4-like composition by heating under UHV to 775 K and to MnO(100) at 1000 K. HREEL spectra for the UHV annealed surfaces are well-resolved, and for the MnO(100)-Mn_3O_4 substrate a second fundamental phonon loss is observed at 55.6 meV as a result of the lower symmetry of the Mn_3O_4 spinel structure. The UHV-annealed MnO(100) surface appears to be more highly ordered since its HREELS phonon loss peaks are better resolved. It is also somewhat reduced, however, resulting in a less intense phonon spectrum with a fundamental loss energy of only 65.1 meV.
© *1996 American Vacuum Society.*

I. INTRODUCTION

The redox properties of transition metal oxide surfaces are important to a number of heterogeneous applications. It is well established that surface oxygen vacancies can play a major role in metal oxide gas adsorption mechanisms,[1] and many studies of single crystal metal oxide substrates have modeled these vacancies as isolated defects in an otherwise unperturbed, bulk-terminated metal oxide lattice. Defects and surface phases involving higher metal oxidation states have been less well characterized at well-defined single crystal surfaces, even for substrates with readily accessible higher metal oxidation states. Manganese, in particular, exhibits formal oxidation states of 2^+, 3^+ and 4^+ in the solid state.[2] These states are sufficiently stable or metastable to allow formation and ultrahigh vacuum (UHV) analysis[3,4] of MnO, α-Mn_2O_3, β-Mn_2O_3, Mn_3O_4 and MnO_2 among the simple oxides. A host of nonstoichiometric, multicomponent and mixed metal oxide valence compounds have also been observed.[2]

From a bulk point of view, manganese monoxide is conceptually simple. MnO possesses low temperature antiferromagnetic properties which have been extensively investigated.[5] The material is, however, paramagnetic above 120 K. Its insulating properties are a result of the localized band structure characteristic of the late cubic 3d transition metal monoxides[6–10] and its high spin d^5 valence ensures a completely filled spin up configuration with no minority, spin down occupancy. The bulk rock salt structure[11] terminates in the thermodynamically stable MnO(100) orientation with no rumpling or reconstruction detectible by low energy electron diffraction (LEED) *I–V* analysis.[12] Thus, the MnO(100) stoichiometric surface structure is particularly straightforward.

The majority of surface studies reported for analysis of the higher manganese oxides and for the oxidation of MnO have been performed on ill-defined powder samples or on thin films oxidized on Mn foils.[3,4,13–15] It is, in principle, possible to distinguish among the simpler manganese oxides with x-ray photoelectron spectroscopy (XPS) by a combination of manganese 2*p* and 3*s* binding energies, satellite structure and O 1*s*/Mn 2*p* intensity ratios. In practice, this generally is only easily accomplished when a single oxide phase is present. Depending upon the oxide(s) present, small changes in stoichiometry, differential surface charging and overlapping features from two or more oxide phases can all complicate the analysis.

This paper reports results for MnO(100) and oxidized MnO(100) single crystal substrates studied by XPS and high resolution electron energy loss spectroscopy (HREELS). Because of the ionic nature of the manganese oxide surface, the HREEL spectrum shows an intense surface phonon structure with multiple phonon excitations characteristic of poorly conducting transition metal oxides. The high symmetry of the MnO rocksalt surface results in a single fundamental phonon loss energy with multiple excitations at integral values of the fundamental phonon loss. Oxidation of the surface leads to the formation of lower symmetry Mn_2O_3 and Mn_3O_4 overlayers, as characterized by XPS. The additional phonon structure is associated with the Mn_3O_4 phase, giving rise to a second fundamental loss in the HREEL spectrum. Mn_2O_3-like overlayers do not show sufficient HREELS reso-

lution to allow for identification of additional loss peaks, although a broad, ill-defined background now forms a substantial fraction of the specularly scattered electron loss spectrum.

II. EXPERIMENT

Surface analysis was carried out in a stainless steel UHV chamber with a base pressure of $\leqslant 3\times 10^{-10}$ Torr maintained by a combination of ion and turbopumping. High resolution electron energy loss spectroscopy was performed with a single pass 127° sector electrostatic analyzer operating at a fixed angle of 60° with respect to the surface normal. All HREEL spectra reported are taken along the specular direction at primary beam energies in the range of 3–8 eV, as noted in the figure captions. Despite low primary beam currents, approximately 1 nA, charging often prevented HREEL spectra of sufficient quality from being obtained at room temperature. Under these conditions, HREELS was acquired at elevated substrate temperatures of 360 K. At these temperatures and HREELS acquisition times of approximately 20 min, no change was detectable in the intensity or peak shapes of either HREEL or XP spectra.

XP spectra were acquired with a Physical Electronics (Φ) 15-225G double pass cylindrical mirror analyzer (CMA). X-ray photoelectron spectra were obtained in pulse count mode at a constant pass energy of 50 eV and were initiated with Mg $K\alpha$ (1253.6 eV) radiation. Data are referenced to the O 1*s* MnO lattice oxygen binding energy, taken to be 529.6 eV, and are in general agreement with values reported in the literature.[3,4,13–15] The UHV system was also equipped with LEED four grid retarding field optics. All data reported here have been taken on MnO(100)-(1×1); no other LEED superstructures were observed.

The MnO single crystal sample, grown by the arc image method, was oriented by Laue back-diffraction and polished with successively finer grades of alumina to a final polishing compound particle size of 0.03 μm. The crystal was nominally square (~5×5×0.2 mm) and was mounted on a stainless steel backing plate either by a thin set of tantalum strips or by nickel mesh. The backing plate was suspended between two tantalum wires, which were heated resistively by a dc power supply. The sample temperature was measured by a Chromel-Alumel thermocouple spot-welded to the stainless steel backing plate. The UHV chamber was baked out at 360 K for approximately 48 h prior to experimentation; samples described "as introduced" have all been subjected to UHV bakeout. Additional sample pretreatment conditions are described in detail below.

III. RESULTS

XP spectra for the MnO(100) crystal, as it was initially introduced into UHV, are shown in Fig. 1. The data are characteristic of MnO, with manganese photoelectron binding energies of 640.8 eV and 652.7 eV for the $2p_{3/2}$ and $2p_{1/2}$ transitions, respectively, and satellite structure at approximately 6 eV (Table I) below the main 2*p* peaks. The satellites are particularly sensitive to the stoichiometry of the oxide,

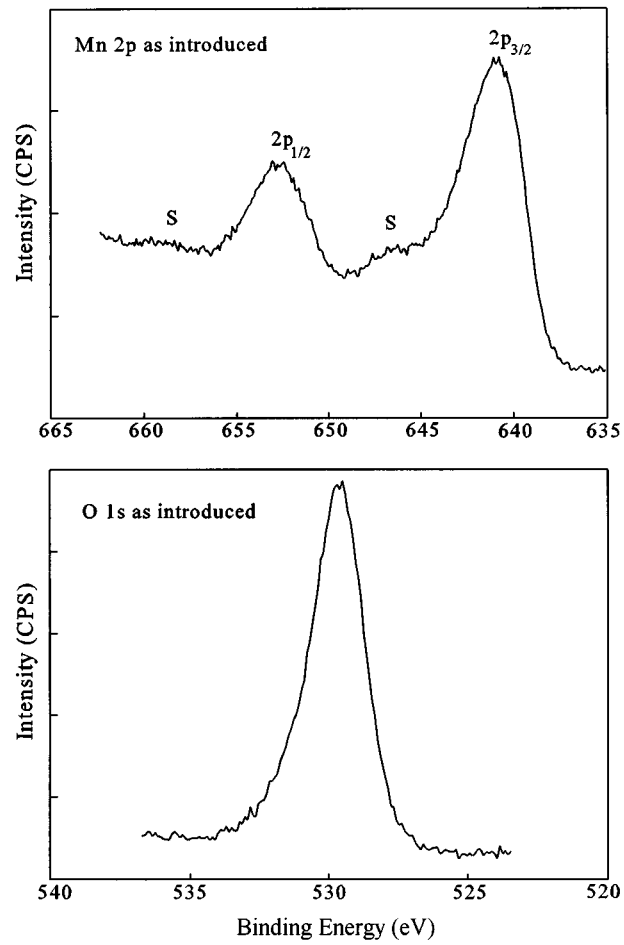

FIG. 1. XPS of the Mn 2*p* and O 1*s* spectral regions. For the Mn 2*p* spectrum, the satellite features are indicated by S.

decreasing in intensity upon either surface oxidation or reduction and disappearing completely in higher oxide phases. The O 1s peak shows a single peak at 529.6 eV with a full width at half-maximum (FWHM) of 2.1 eV due to the oxygen lattice but with some tailing to the higher binding energy side. Assuming Gaussian peak shapes for two peaks at 529.6 and 531.2 eV, a curve fit of the O 1*s* data in Fig. 1 estimates the maximum amount of intensity attributable to the higher binding energy peak at 17%. Carbon impurities were below the detection limits of the XPS.

The HREEL spectrum of the "as introduced" sample is shown in the top panel of Fig. 2 and is decidedly uncharacteristic of an uncontaminated, well-ordered rocksalt oxide. No phonon structure inherent to the oxide surface is detectable. Instead the spectrum is dominated by a broad loss peak at 40 meV attributed to nonstoichiometric oxygen species. We suggest this feature is characteristic of lattice oxygen species adjacent to cation vacancies and/or cation vacancy-interstitial pairs. Cation defects in nonstoichiometric metal oxides can result in a net oxidation of the adjacent O^{2-} lattice anions and the relatively low loss energy of the species in the HREEL spectrum is consistent with the formation of O^{-}-like species. The O 1*s* XPS for the as introduced

TABLE I. XPS of MnO(100) and oxidized MnO(100) surfaces (binding energies in eV) O1s/Mn 2*p* ratio uses entire 2*p* intensity.

	Mn $2p_{3/2}$	Satellite ($2p_{3/2}$)	Mn $2p_{1/2}$	Satellite ($2p_{1/2}$)	O/Mn Intensity	O 1*s* [a] FWHM
MnO(100) as introduced	640.8	647	652.7	658.7	0.28	2.1
MnO(100) 30 min O_2 anneal at 625 K	640.6	646.5	652.5	658.6	0.24	2.9
MnO(100)Mn_2O_3 150 min O_2 anneal at 625 K	641.1	⋯	652.8	⋯	0.41	2.6
MnO(100)Mn_3O_4 O_2 anneal + 775 K UHV anneal	641.6	⋯	653.3	⋯	0.35	3.4
MnO(100) regenerated at 1000 K under UHV	640.7	647	652.3	658.5	0.22	2.7

[a]O 1*s* binding energy set to 529.6 eV as internal calibration.

MnO(100) supports this assignment since the nonstoichiometric "tailing" feature at 531.2 eV is identical in binding energy to that previously observed for O^- in metal monoxide thin films.[16] Thus, although the XPS gives evidence for a reasonably clean and stoichiometric MnO(100) surface, the HREEL spectrum indicates that the surface quality is actually quite poor. Small amounts of adsorbed carbon monoxide (175 meV) and carbonate (~220 meV) are also evident, indicating that the HREEL spectrum is more sensitive than is the C 1*s* XPS in detecting these species. Particularly noteworthy is the absence of hydroxyl loss features, typically found over the range of 440–470 meV, depending upon the degree of hydrogen bonding.

Annealing the MnO substrate under 5×10^{-7} Torr O_2 at 625 K gradually increases the oxygen content of the near-surface region. The change is slow and the initial result of the low temperature oxygen anneal is to remove the low level of carbon contaminants and to order the MnO(100) surface. Heating the MnO substrate for 30 min does not change the Mn 2*p* (Fig. 3) or O 1*s* XP spectra detectably with the exception that the O 1*s* peak is broadened somewhat to 2.9 eV FWHM. XPS peak positions (Table I) and satellite structure remain constant, and the surface still shows the MnO (1x1) LEED pattern. A slight decrease in the O 1*s*/Mn 2*p* intensity ratio occurs, presumably due to desorption of surface carbonates and to MnO surface reduction through reactions with carbon-containing adsorbates.

The HREEL spectrum, however, changes considerably as the surface begins to develop the Fuchs–Kliewer phonon loss features characteristic of ionic rocksalt materials. A fundamental phonon loss is observed at 70.9 meV with additional structure to higher loss energies. The phonons, which are surface analogs of the bulk transverse optical phonon, have large dipole moments due to the out of phase cation–anion oscillatory motion. The HREEL spectrum of a rocksalt monoxide surface thus generally shows intense single loss features with additional losses at integral multiples of the single-loss peaks and with intensities decreasing in a Poisson distribution. While the Fuchs–Kliewer phonon spectrum of MnO has not previously been reported, the single loss phonon energy is in good agreement with those of the related systems NiO [70.5 meV (Ref. 17)] and CoO [68.9 meV (Ref. 18)].

Based on the 70.9 meV single loss energy, multiple losses in the MnO(100) HREEL spectrum are marked with asterisks in Fig. 2. A double loss feature is evident at 142 meV and, although the spectrum is too ill-defined to resolve individual loss features for higher multiple scattering events, spectral tailing is consistent with the expected Poisson intensity distribution of the loss function. In addition to the poor spectral resolution, the net phonon intensity is less intense than comparable HREEL spectra of the related CoO (Ref. 17), NiO (Ref. 18) and ZnO (Ref. 19) surfaces where for stoichiometric surfaces the single loss phonon is typically 60%–80% as intense as the elastic peak.

Heating the MnO(100) surface under 5×10^{-7} Torr O_2 at 625 K for extended periods gradually increases the O/Mn XPS intensity ratio until after 2.5 h the ratio has increased by 1.5 over the initial MnO(100) as introduced surface value. The 2*p* satellite feature characteristic of the monoxide also gradually disappears and the 2*p* binding energies shift to higher values. Both the change in O/Mn XPS intensity ratio and the 2*p* profile suggest the formation of Mn_2O_3 as has previously been observed during the oxidation of MnO thin films grown on manganese foils.[15] However, little change is observed in the HREEL spectrum, which remains ill-defined with a few broad features at energies similar to that of the MnO(100) Fuchs–Kliewer phonon spectrum. A representative HREEL spectrum for MnO(100) extensively annealed under 5×10^{-7} Torr O_2 at 625 K is given in the bottom panel of Fig. 2. The spectrum was acquired on a MnO(100) substrate annealed for 2.5 h under O_2 followed by a 1 h UHV

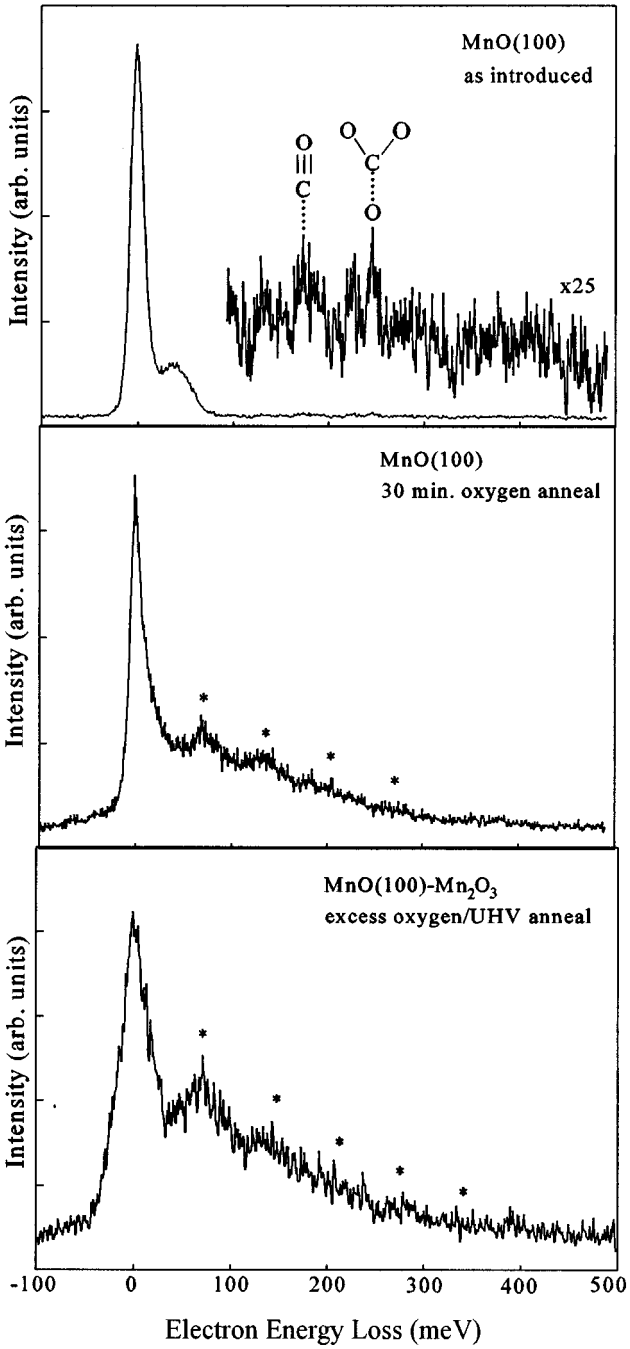

FIG. 2. HREEL spectra of MnO(100) as introduced, MnO(100) after a brief oxygen anneal and MnO(100)-Mn_2O_3 formed after extended oxygen anneal, as described in the text. The primary electron beam scattering energy is 3.2 eV for the as introduced sample and 3.4 eV for the oxygen-annealed samples. Asterisks mark the phonon loss progression.

anneal at 625 K in an attempt to improve the surface order. The phonon spectrum is comparable to that observed for the substrate with XPS characteristics of MnO produced after the brief, 30 min O_2 anneal with the exception that the phonon to elastic peak intensities have increased substantially with extended O_2 anneal and the peak resolution has degraded even further.

If subjecting the MnO(100) substrate to oxidizing conditions results in surface oxidation, it might be expected that reducing conditions would lead to a transition to less oxidized manganese oxides. The Mn_2O_3-like overlayer appears to be stable under UHV, at least over the course of several days, although the mobility of manganese and oxygen ions is probably insufficient to ensure that all but the outermost layer of the manganese oxide surface is affected. Heating the substrate under UHV for periods of 1 h likewise brings very small changes until a substrate temperature of 775 K is reached. At this point, the HREEL spectrum sharpens (Fig. 4) considerably to yield detectable phonon losses from the 70.9 meV fundamental loss down to the fourth loss multiple. In addition, a second phonon mode has appeared as a distinct loss peak at 55.6 meV, indicating the formation of an oxide with well-defined order but with a symmetry lower than that

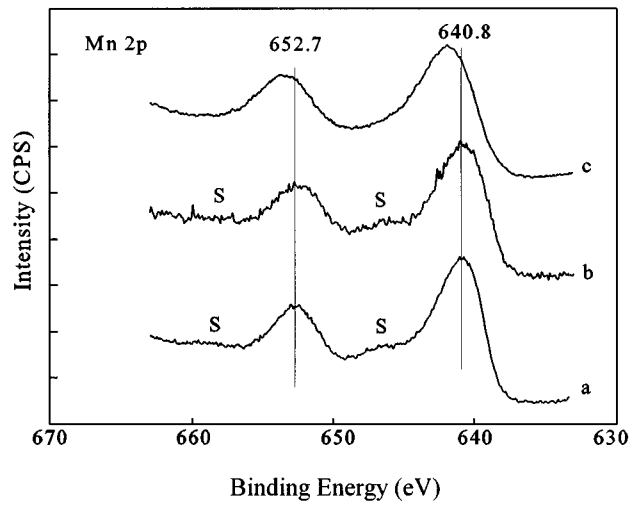

FIG. 3. XP 2*p* spectra for (a) MnO(100) as introduced, (b) MnO(100) after 30 min oxygen anneal and (c) MnO(100)-Mn_2O_3 formed after extended oxygen anneal.

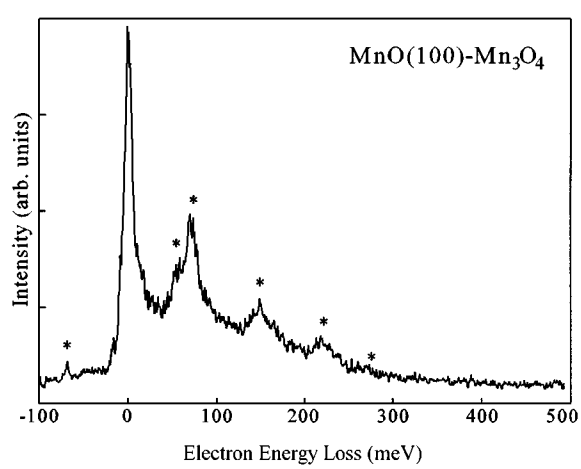

FIG. 4. HREEL spectrum for the MnO(100)-Mn_3O_4 surface formed after over-oxidizing the surface to Mn_2O_3 and reducing it under UHV at 775 K. Phonons positions are marked with asterisks. The primary electron beam energy is 5.0 eV.

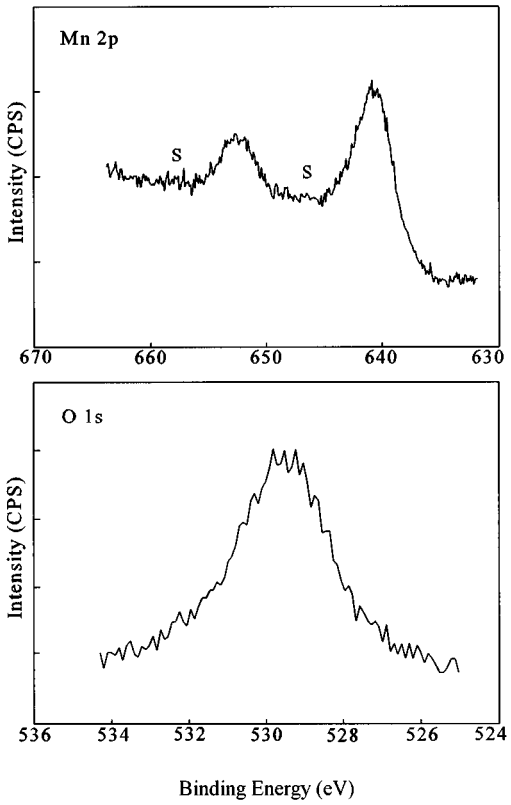

FIG. 5. XPS of the Mn 2*p* and O 1*s* regions of MnO(100) prepared by over-oxidizing the near surface to Mn_2O_3 and subsequently reducing the surface in a series of UHV anneals under increasing substrate temperature. The highest and final anneal temperature for this surface is 1000 K for 10 min.

expected of the cubic MnO(100). XPS O/Mn ratios are 1.3 times the value of the initial MnO(100) surface. This and XPS binding energies (Table I) suggest that the oxide formed is Mn_3O_4. The HREEL spectrum is similar to that observed for the related system of Co_3O_4 thin films grown epitaxially on CoO(100). HREEL spectra for well-defined orientations of single crystal have not been reported for these spinel materials.

Upon continued increase in substrate anneal temperature, a surface with XPS and HREELS properties of MnO(100) (Fig. 5), and uncontaminated by higher oxides, was observed after annealing at 1000 K for 10 min. Lower substrate temperatures appear to leave some higher manganese oxidation state contamination in the near-surface region, but reduction at 1000 K is rapid. The Mn $2p_{3/2}$ and $2p_{1/2}$ XPS satellites characteristic of the monoxide are again found at approximately 6 eV higher binding energy than the main 2*p* peaks. However, the satellites are not as well developed as expected for stoichiometric MnO and the O/Mn XPS intensity ratio is only 80% of the value observed for the as introduced sample, indicating that the surface has been somewhat over-reduced.[20]

Because the defects impart conductivity to the oxide, the phonon spectrum is substantially damped, resulting in a low intensity but otherwise well-resolved spectrum of MnO with

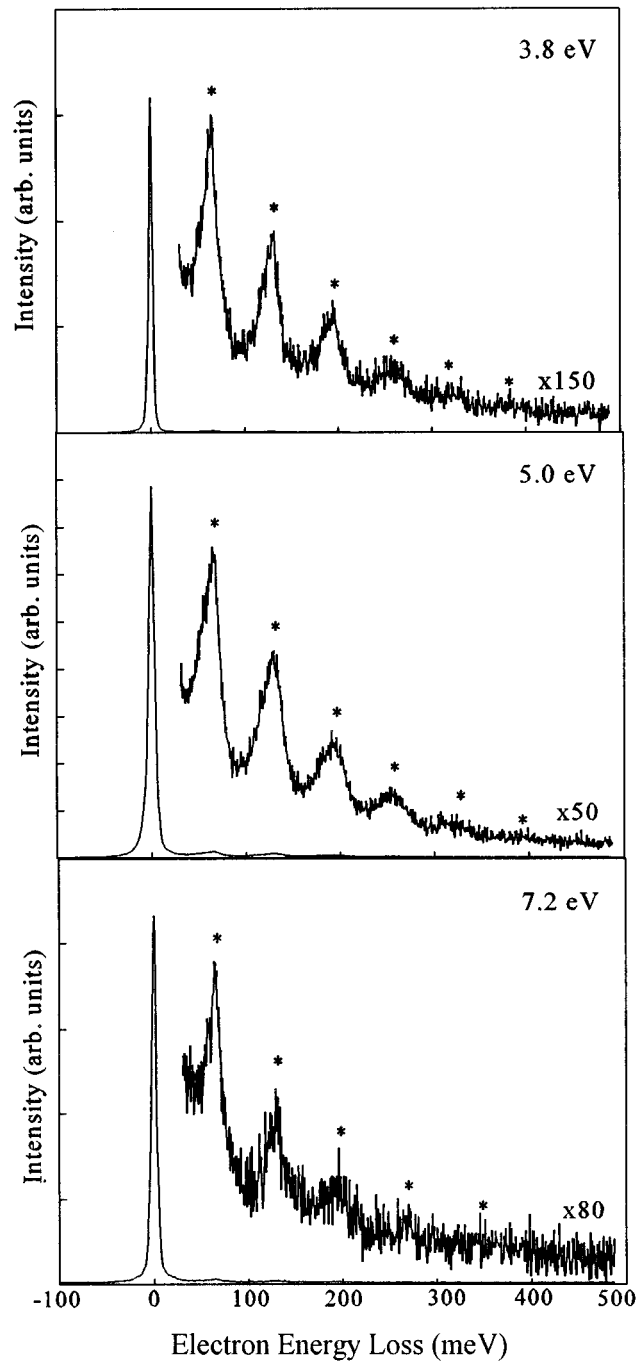

FIG. 6. HREEL spectra for several primary beam energies taken on the MnO(100) surface prepared by over-oxidizing the near surface to Mn_2O_3 and subsequently reducing the surface in a series of UHV anneals under increasing substrate temperature. The highest and final anneal temperature for this surface is 1000 K for 10 min. Asterisks mark the phonon progression.

Fuchs–Kliewer multiple phonon excitations out to the sixth multiple (Fig. 6). The fundamental loss energy is only 65.1 meV, a shift from the 70.9 meV phonon energy observed for the MnO(100) HREEL spectrum of Fig. 2, which could be attributable to the nonstoichiometric nature of the over-reduced MnO(100). Lower loss energies have previously

been observed for NiO(100) (Ref. 21) and NiO(111) (Refs. 21 and 22) thin oxide film grown nickel metal substrates as well as NiO(100) single crystal substrates that had been reduced under H_2.[17]

IV. DISCUSSION

Because of the number of oxidation states available to manganese in the solid state, the surface properties of manganese oxides are potentially complex. Particularly under redox conditions at substrate temperatures that allow for cation migration within the near-surface region, the manganese oxide surface can support a range of manganese oxidation states and oxide phases. Since near-surface diffusion is expected to play a role, the species formed are not necessarily the thermodynamically most stable ones and several oxidation states may be present even under seemingly straightforward and simple surface pretreatment conditions. These states and interconversion among them will be important in determining manganese oxide chemisorption and surface chemical reactivity. This is true even when single crystal substrates are employed since the simpler oxides (MnO, Mn_3O_4 and Mn_2O_3) are all closest packed in oxygen and differ primarily in the filling of octahedral and tetrahedral sites with Mn^{2+}/Mn^{3+} cations.

MnO(100) can support several higher oxide phases in sufficient amounts and well enough ordered to yield characteristic XPS and HREELS data indicating the oxide is present and even dominant in concentration in the near-surface region. By adjusting the substrate temperature and oxidizing/reducing surface pretreatment conditions it is possible to select the dominant oxide form, MnO, Mn_2O_3 or Mn_3O_4, present at the MnO(100) surface. It is, however, difficult to isolate a single oxide phase, free of other oxide components once the substrate has been exposed to O_2 and/or heated above approximately 600 K.

In the present set of experiments, the as introduced MnO(100) sample appears by XPS to be stoichiometric monoxide in the near-surface region although HREELS shows that the surface itself is contaminated with adsorbates that survive the 360 K UHV bakeout. Brief O_2 anneals remove the adsorbate but have the potential of introducing significant quantities of higher manganese oxides. Annealing under 5×10^{-7} Torr O_2 at 625 K generates a stable Mn_2O_3 overlayer in a roughly commensurate epitaxy with the underlying MnO(100). The oxide continues to produce a (1×1) LEED pattern relative to the MnO(100) substrate, although the quality of LEED on the single crystal substrate was never ideal because of the poor conductivity of the surface. Thus, fractional order diffraction features cannot be ruled out for the oxidized MnO surfaces and no information was extracted on the location of the cations in the oxidized surface phase. However, the LEED results do indicate that no extensive faceting has occurred during oxidation. The HREEL spectra indicate that the surface is not completely homogeneous.

Upon heating under UHV, surface reduction was effected and the following sequence was observed:

$$Mn_2O_3 \xrightarrow{775\ K} Mn_3O_4 \xrightarrow{1000\ K} MnO.$$

While thermodynamic considerations are obviously important in determining the stability of a given oxide phase at a given set of O_2 partial pressure/temperature conditions, kinetic factors are also important. It is therefore possible to over reduce the surface or to produce a surface with mixed oxide composition by this route.

V. CONCLUSION

The surface of a MnO(100) single crystal can be selectively oxidized or reduced by annealing under appropriate low pressure O_2 or UHV conditions. Oxide phases that are predominantly Mn_2O_3, Mn_3O_4 or MnO are observed in roughly epitaxial relation to the MnO(100) substrate. The phases are easily intermixed and it is difficult to isolate pure epitaxial layers uncontaminated by other oxides. The ready formation and intermixture of these species imply that the redox properties of manganese oxide surfaces will be important in their surface chemical reactivity and gas adsorption characteristics.

ACKNOWLEDGMENTS

The authors are grateful for support from NSF under the primary Grant No. CHE9220341 and for access to equipment obtained under NSF Grant No. CHE9508600.

[1]V. E. Henrich and P. A. Cox, *The Surface Science of Metal Oxides* (Cambridge, New York, 1994).
[2]W. Levason and C. A. McAuliffe, Coord. Chem. Rev. **7**, 353 (1972).
[3]M. Oku, K. Hirokawa, and H. Ikeda, J. Electron Spectrosc. Relat. Phenom. **7**, 465 (1975).
[4]J. S. Foord, R. B. Jackman, and G. C. Allen, Phil. Mag. A **49**, 657 (1984).
[5]C. Kittel, *Introduction to Solid State Physics*, 6th ed. (Wiley, New York, 1986), p. 442.
[6]A. Fujimori and F. Minami, Phys. Rev. B **30**, 957 (1984).
[7]A. Svane and O. Gunnarsson, Phys. Rev. Lett. **65**, 1148 (1990).
[8]Z.-X. Shen, J. W. Allen, P. A. P. Linberg, D. S. Dessau, B. O. Wells, A. Borg, W. Ellis, J. S. Kang, S.-J. Oh, I. Lindeau, and W. E. Spicer, Phys. Rev. B **42**, 1817 (1990).
[9]R. J. Lad and V. E. Henrich, Phys. Rev. B **38**, 10 860 (1988).
[10]S.-P. Jeng, R. J. Lad, and V. E. Henrich, Phys. Rev. B **43**, 11 971 (1991).
[11]W. D. Johnston and R. R. Heikes, J. Am. Chem. Soc. **78**, 3255 (1956).
[12]M. Prutton, J. A. Walker, M. R. Welton-Cook, R. C. Felton, and J. A. Ramsey, Surf. Sci. **89**, 95 (1979).
[13]M. Oku and K. Hirokawa, J. Electron Spectrosc. Relat. Phenom. **8**, 475 (1976).
[14]U. Linder and H. Papp, Appl. Surf. Sci. **32**, 75 (1988).
[15]V. DiCastro and G. Polzonetti, J. Electron Spectrosc. Relat. Phenom. **48**, 117 (1989).
[16]J. P. S. Badyal, X. Zhang, and R. Lambert, Surf. Sci. Lett. **225**, L15 (1990).
[17]K. W. Wulser and M. A. Langell, Surf. Sci. **314**, 385 (1994).
[18]M. H. Nassir and M. A. Langell, Solid State Commun. **92**, 791 (1994).
[19]H. Ibach, Phys. Rev. Lett. **24**, 1416 (1970).
[20]G. A. Carson, M. H. Nassir, and M. A. Langell, Mater. Res. Soc. Symp. Proc. **335**, 163 (1995).
[21]M. A. Langell, C. L. Berrie, M. H. Nassir, and K. W. Wulser, Surf. Sci. **320**, 25 (1994).
[22]M. A. Langell and M. H. Nassir, J. Phys. Chem. **99**, 4162 (1995).